ELSEVIER

Carbohydrate Research 283 (1996) 111–127

CARBOHYDRATE RESEARCH

Structural studies of the lipopolysaccharide O-antigen and capsular polysaccharide of *Vibrio anguillarum* serotype O:2 [1]

Irina Sadovskaya [a], Jean-Robert Brisson [a], Eleonora Altman [a,*], Lucy M. Mutharia [b]

[a] *Institute for Biological Sciences, National Research Council of Canada, Ottawa, Ontario, K1A 0R6, Canada*
[b] *Department of Microbiology, College of Biological Sciences, University of Guelph, Guelph, Ontario, N1G 2W1, Canada*

Received 9 August 1995; accepted 13 November 1995

Abstract

Vibriosis caused by *Vibrio anguillarum* affects salmonid and marine fish species worldwide and is considered to be one of the most serious threats to the success of commercial fish farming. In the course of this study, it was found that *V. anguillarum* serotype O:2 strains produce an acidic capsular polysaccharide having the identical structure to that of the O-chain polysaccharide. One-dimensional and two-dimensional nuclear magnetic resonance techniques, together with partial hydrolysis and various specific modifications, were used to determine the structure of these polysaccharides. It is proposed that both O-chain and capsular polysaccharide of *V. anguillarum* serotype O:2 are composed of linear tetrasaccharide repeating units having the following structure, in which Glc2NAc3NAN represents 2-acetamido-3-amino-2,3-dideoxy-D-glucuronamide, Man2NAc3AmA is 3-acetamidino-2-acetamido-2,3-dideoxy-D-mannuronic acid, Am represents an acetamidino group, $Gal(NAc)_2A$ is 2,3-diacetamido-2,3-dideoxy-L-galacturonic acid, $Bac(NAc)_2$ is 2,4-diacetamido-2,4,6-trideoxy-D-glucose (*N*,*N*′-diacetylbacillosamine) and Fo is formyl.

$$[\rightarrow 4)\text{-}\beta\text{-D-}Glc_p2NAc3NAN(1\rightarrow 4)\text{-}\beta\text{-D-}Man_p2NAc3AmA(1\rightarrow 4)\text{-}\alpha\text{-L-}Gal_p(NAc)_2A(1\rightarrow 3)\text{-}\beta\text{-D-}Bac_p(NAc)_2(1\rightarrow]_n$$
$$\text{Fo-L-Ala}$$

* Corresponding author.

[1] This work was supported by funding from the Canadian Bacterial Diseases Network (Federal Networks of Centres of Excellence Program). Presented in part at the XVII International Carbohydrate Symposium, Ottawa, Canada, July 17–22, 1994. This is National Research Council Publication Number 39501.

SSDI 0008-6215(95)00398-3

Keywords: *Vibrio anguillarum*; Capsular polysaccharide; O-Antigen; Structure; NMR spectroscopy

1. Introduction

Vibrio anguillarum is a Gram-negative bacterium that is associated with severe outbreaks of vibriosis in salmonid and marine species worldwide [1]. The lipopolysaccharide (LPS) is thought to be a major virulence factor of *Vibrio* species and a serotyping scheme consisting of 10 distinct O-antigenic serotypes has been developed [2,3].

The most common causes of vibriosis in salmonid cultures worldwide are serotype O:1 strains of *V. anguillarum*, while serotype O:2 strains are more common in European aquaculture [4].

A bivalent vaccine composed of killed bacterial preparations of *V. anguillarum* O:1 and *V. ordalii* O:2, indistinguishable by western immunoblotting using rabbit polyclonal serum from *V. anguillarum* serotype O:2 [5], has been largely effective in reducing incidence of disease.

However, serious outbreaks of vibriosis have occurred in Atlantic salmon, in New Brunswick, despite prior vaccination of these fish with a bivalent vaccine. The situation with New Brunswick cage-culture suggests that antigens other than LPS may contribute to immune protection against vibriosis. In addition, it demonstrates the need for the systematic structural characterization of the LPS from *V. anguillarum* and *V. ordalii* in order to provide the immunochemical rationale for the serotyping of *Vibrio* species and for the development of protective fish vaccines.

Recently, alterations in the length of O-chain polysaccharide and a formation of extracellular material, possibly a capsule, have been described for *Vibrio* species grown in the presence of rainbow trout blood [6].

Although presence of capsular antigens in *V. anguillarum* has been reported [7], their role in the pathogenicity of vibrios is largely unknown.

In the present investigation we describe the isolation and structural analysis of capsular polysaccharide and O-chain polysaccharide from *V. anguillarum* serotype O:2.

2. Results

Isolation and characterization of the O-chain polysaccharide and capsular polysaccharide (PS1).—Cells of *V. anguillarum* were grown under aerobic conditions, washed with saline, and incubated in phosphate buffer containing egg-white lysozyme. The capsular polysaccharide (PS1) was recovered by precipitation with ethanol [8] and purified by gel-filtration chromatography on a column of Sephadex G-100. The void volume fraction was collected and applied to a column of Sepharose 6B. The PS1 eluted as a broad peak (K_{av} 0.45) and was homogeneous with respect to neutral glycose and aminoglycose. It had $[\alpha]_D$ −109.1° (*c* 0.4, water). Anal. found: C, 39.5; H, 5.3; N, 12.17%.

The lipopolysaccharide was extracted from the saline-washed cells by the phenol–

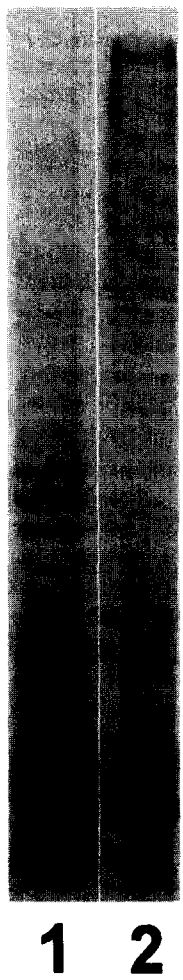

Fig. 1. SDS–PAGE (12.5%) pattern of LPS from *Vibrio anquillarum* serotype O:2 strain ATCC 19264 (lane 1) and *Salmonella enteritidis* strain 27655-36 (lane 2).

water method [9], and the aqueous-phase LPS was purified by repeated centrifugation. The silver-stained profiles of purified aqueous-phase LPS gave a pattern typical of the smooth type although the bands representing LPS with shorter O-chains were more pronounced than in the SDS-PAGE banding pattern of *Salmonella enteritidis* (Fig. 1). Partial hydrolysis of the S-type LPS with hot dilute acetic acid gave an insoluble lipid A, and gel-filtration chromatography of the concentrated water-soluble products on Sephadex G-100 afforded a high molecular weight glucan (K_{av} 0, 8%), O-chain (K_{av} 0.27, 18%) and a core oligosaccharide (K_{av} 0.68, 27%). The O-chain had $[\alpha]_D$ −79.3° (*c* 0.7, water). Anal. found: C, 43.07; H, 5.50; N, 10.29; ash, 0%.

Based on the results of the monosaccharide and methylation analyses and the NMR evidence, the high molecular mass material was identified as a branched α-(1 → 4)-linked

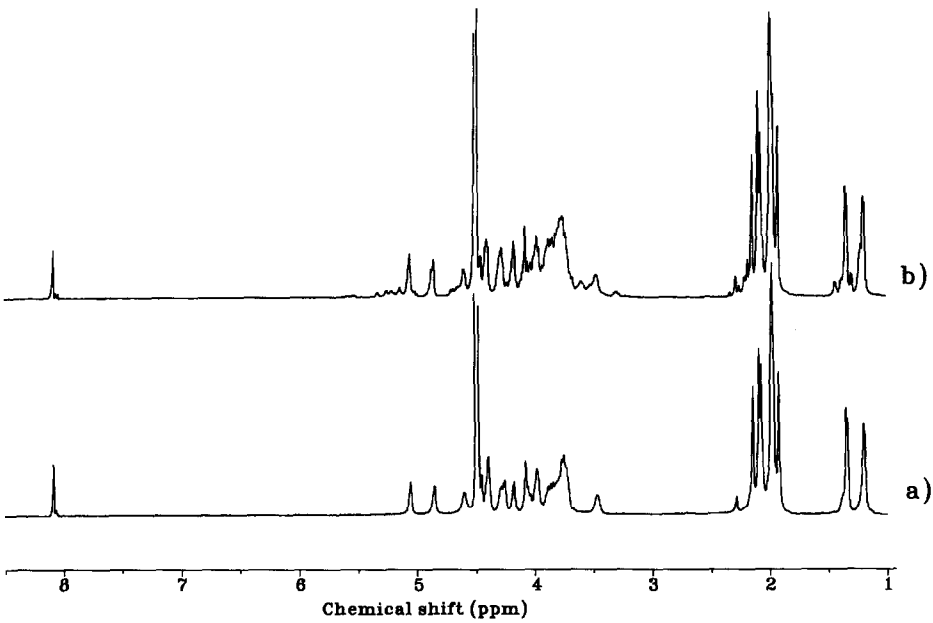

Fig. 2. The ^{1}H NMR spectra of the PS1 (a) and O-chain polysaccharide (b) from *V. anguillarum* serotype O:2 recorded at 50 °C in D_2O at pH 7.0.

glucan with α-(1 → 6)-linked branches occurring every six glucose residues. A similar glycogen-type structure was previously found in *Vibrio cholerae* serotype O:2 [10]. This material was not further investigated.

Composition analysis of the PS1 and the O-chain polysaccharide.—Hydrolysis of PS1 with 10 N HCl afforded 2,4-diamino-2,4,6-trideoxy-D-glucose as the only GLC–MS-detected component. In addition, 2,3-diamino-2,3-dideoxyhexose was identified in the hydrolysis products of the carbodiimide-reduced PS1. Compositional analysis of the O-chain polysaccharide revealed presence of 2,4-diamino-2,4,6-trideoxy-D-glucose and glycoses characteristic of the core component, D-glucose, D-galactose, and L-*glycero*-D-*manno*-heptose, in approximate molar ratio of 0.8:2.0:1.0:2.8. Amino acid analyses confirmed the presence of L-alanine (L-Ala) in both polysaccharides.

NMR analysis.—The ^{1}H NMR analysis and ^{13}C NMR spectra of the O-chain polysaccharide and PS1 were identical at pH 7.0, which made it possible to assume that the two polysaccharides had the same structure (Fig. 2). Due to its higher homogeneity and the absence of the minor signals belonging to the core region, PS1 was chosen for a detailed structural and NMR analysis.

Examination of the ^{13}C NMR spectrum of PS1 (Fig. 3) indicated the presence of four anomeric ^{13}C resonances at 102.2, 101.0, 99.8, and 98.6 ppm, and nine signals of nitrogen-carrying carbons at 44–58 ppm, suggesting an unusual composition of the repeating unit. In addition, six acetamido methyl group resonances at 22.9–23.3 ppm, together with the numerous carboxyl resonances in the low-field region (174.4–176.7 ppm), indicated the presence of at least six *N*-acetyl groups. Characteristic ^{13}C signals

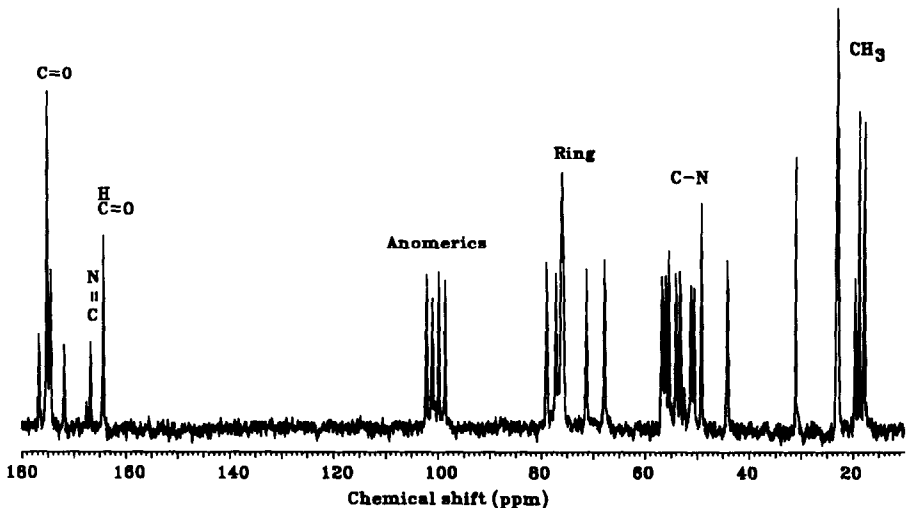

Fig. 3. 125-MHz ^{13}C NMR spectrum of the PS1 recorded at 50 °C in D_2O at pH 7.0.

Table 1
Proton chemical shifts for PS1 [a,e], PS2 [a], and OS2 [b,e] of *V. anguillarum* serotype O:2 [c,d]

Residue	Compd	H-1	H-2	H-3	H-4	H-5	H-6	$=CCH_3$			NH			
								2	3	4	2	3	4	6
a	PS1	5.06	4.40	4.27	4.17	4.07		1.98	2.06		7.88	6.92		
	PS2	5.06	4.39	4.27	4.15	4.06		1.98	2.07		7.83	6.90		
	OS2	5.13	4.45	4.32	4.17	4.12		2.00	2.09		7.83	6.96		
b	PS1	4.85	4.45	3.99	3.88	3.76		2.08	2.14		8.42	8.81		
	PS2	4.84	4.06	4.37	3.75	3.78		1.89	2.07		7.78	8.29		
	OS2	4.87	4.48	3.99	3.94	3.78		2.09	2.18		8.50	8.95		
c	PS1	4.59	3.72	4.05	3.84	3.97		1.97			7.95	8.11		8.15, 7.52
	PS2	4.59	3.72	4.05	3.86	3.97		1.96			7.89	8.13		8.13, 7.52
	OS2	4.55	3.69	3.95	3.61	3.79		1.97			7.83	8.11		
d	PS1	4.28	3.80	3.75	3.72	3.46	1.19	1.92		1.96	8.24		8.29	
	PS2	4.30	3.80	3.75	3.73	3.46	1.19	1.92		1.96	8.23		8.29	
β	OS2	4.61	3.93	3.80	3.82	3.61	1.22	1.96		2.00	8.32		8.38	
α	OS2	5.06	4.14	3.98	3.84	4.04	1.18	1.96		2.00	8.39		8.45	
FoNAla	PS1		4.39	1.34	8.08						8.19			
FoNAla	PS2		4.40	1.34	8.08						8.19			
AcNAla	OS2		4.21	1.30		2.00					8.14			

[a] Recorded at 50 °C in D_2O, 10 mM phosphate buffer at pH 7.0.
[b] Recorded at 27 °C in D_2O at pH 7.0.
[c] NH protons spectra were recorded at 27 °C on 90% H_2O–10% D_2O at pH 7.0.
[d] Internal acetone resonance set at 2.225 ppm.
[e] Amidino ($C=N^+H_2$) signals NH-3**b**′ and NH-3**b**″ at 8.65 and 8.36 ppm for PS1 and at 8.65 and 8.37 ppm for OS2.

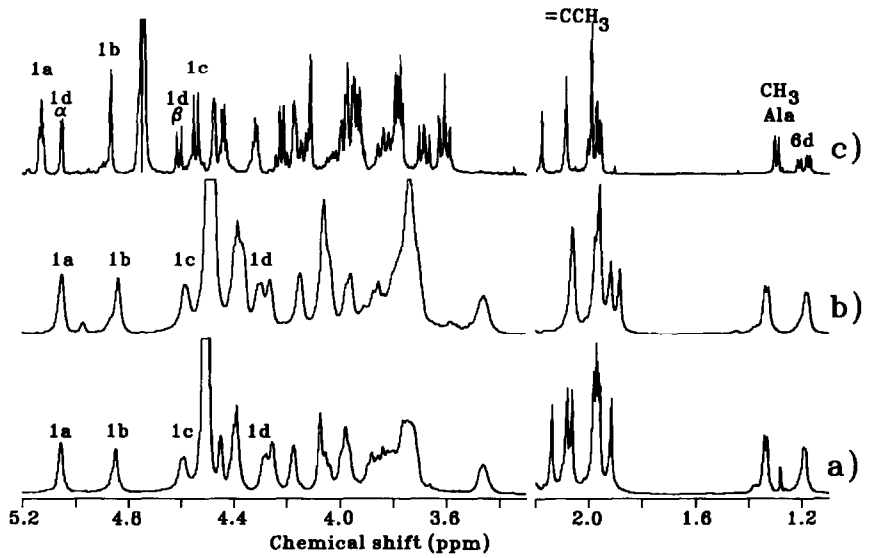

Fig. 4. 600 MHz ^{1}H NMR spectrum in D_2O at pH 7.0 of (a) PS1 at 50 °C, (b) PS2 at 50 °C and (c) OS2 at 27 °C.

of *C*=N (166.7 ppm) and *C*H_3–C=N (19.7 ppm) groups belonged to the acetamidino group [10–12]. A ^{13}C signal at 164.3 ppm indicated presence of an *N*-formyl group. In the high-field region, two methyl group signals were present at 18.9 and 17.9 ppm.

The ^{1}H resonances of PS1 were assigned using a 2D proton chemical shift correlated spectroscopy (COSY) and a total correlated spectroscopy (TOCSY) (Table 1). The anomeric protons of four glycose residues were designated **a–d**, according to the decreasing order of their chemical shifts in the ^{1}H NMR spectrum of PS1 (Fig. 4, see also Fig. 5). Assignment of the ^{13}C resonances (Table 2) was carried out by direct correlation of the ^{1}H resonances with the ^{13}C resonances in an heteronuclear ^{13}C–^{1}H chemical shift correlation HMQC (heteronuclear quantum coherence) experiment. The heteronuclear multiple bond correlated (HMBC) experiment served to correlate CH_3 proton resonances with the corresponding C=O and C=N resonances via long-range $^{3}J_{C,H}$ connectivities (Table 2).

Most NH resonances of PS1 were assigned on the basis of their large coupling constant with the ring protons H–C–N–H (9–10 Hz) via COSY and TOCSY experiments on the samples in 90% H_2O–10% D_2O. The methyl groups of the *N*-acetyl groups were assigned on the basis of a strong nuclear Overhauser effect (NOE) between NH and CH_3 resonances, within the *N*-acetyl group (Fig. 6). The HMQC experiment was then employed to assign the corresponding *C*H_3 signals (22–24 ppm) in the ^{13}C spectrum (Table 2).

Partial hydrolysis of PS1, followed by *N*-acetylation, afforded a tetrasaccharide OS2, as a major product (see Experimental section for details), indicating a relative acid lability of 2,4-diamino-2,4,6-trideoxy-D-glucose (Fig. 7). Complete assignment of the ^{1}H and ^{13}C spectra of OS2 was performed as outlined above for PS1 (Tables 1 and 2). The

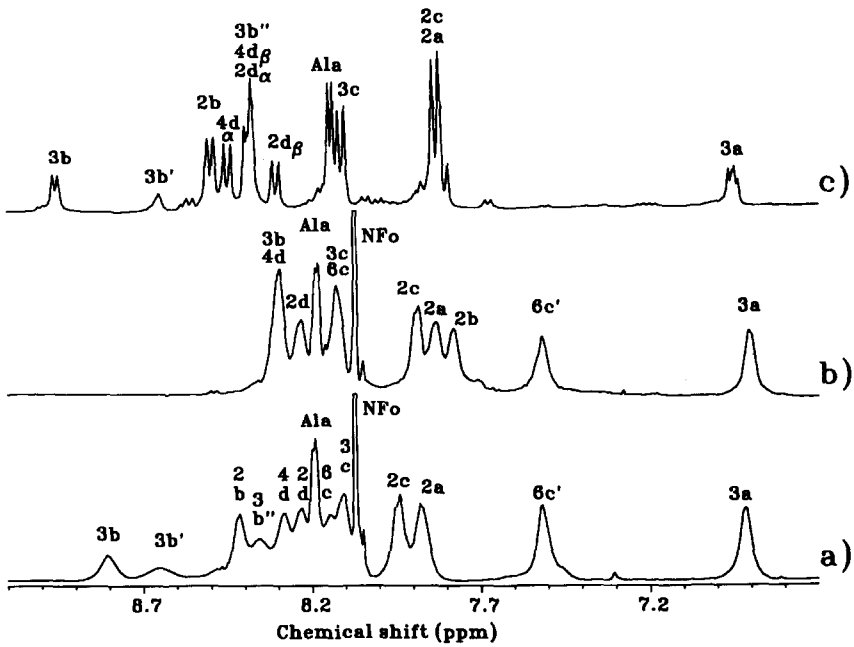

Fig. 5. 600-MHz ^{1}H NMR spectrum of the NH region of (a) PS1, (b) PS2, and (c) OS2 at 27 °C in 90% H_2O–10% D_2O at pH 7.0. NFo = *N*-formyl. The two NH signals of the protonated amidino group ($C=N^+H_2$) are designated 3**b**′ and 3**b**″. The two resonances for the NH_2 protons at 6**c** are labelled 6**c** and 6**c**′.

Table 2
^{13}C chemical shifts for PS1 [a], PS2 [a], and OS2 [b] of *V. anguillarum* serotype O:2 [c]

Residue	Compd	C-1	C-2	C-3	C-4	C-5	C-6	=CCH$_3$			=C		
								2	3	4	2	3	4
a	PS1	98.58	44.17	50.67	76.15	67.82	175	22.97	23.29		175	175	
	PS2	98.63	44.24	50.71	76.10	67.84	175	22.98	23.31		175	175	
	OS2	98.71	44.15	50.68	76.70	67.86	175.3	23	23.33		175	175	
b	PS1	99.81	51.24	55.47	76.15	77.20	175	22.87	19.65		176.7	166.7	
	PS2	100.06	52.45	52.22	76.67	77.23	175	22.82	22.82		176.1	175	
	OS2	99.98	50.97	55.39	75.67	79.16	176.0	23	19.72		176.7	166.7	
c	PS1	102.17	54.13	53.29	75.78	75.98	171.8	23.17			175		
	PS2	102.27	54.19	53.50	76.00	76.10	171.9	23.19			175		
	OS2	102.29	54.10	55.29	70.61	78.35	176.0	23.18			175		
d	PS1	101.04	56.78	78.97	56.06	71.29	17.87	23.17		23.07	174.4		175
	PS2	101.09	56.81	79.29	56.09	71.28	17.87	23.18		23.09	174.5		175
β	OS2	95.59	57.85	77.21	56.13	71.65	17.76	23		23	175		175
α	OS2	91.69	55.39	74.69	56.13	67.13	17.73	23		23	175		175
FoNAla	PS1	175	49.20	18.90	164.3								
FoNAla	PS2	175	49.22	18.91	164.3								
AcNAla	OS2	176.5	50.69	17.85	175	23							

[a] Recorded at 50 °C in D_2O, 10 mM phosphate buffer at pH 7.0.
[b] Recorded at 27 °C in D_2O at pH 7.0.
[c] Internal acetone methyl resonance set at 31.07 ppm.

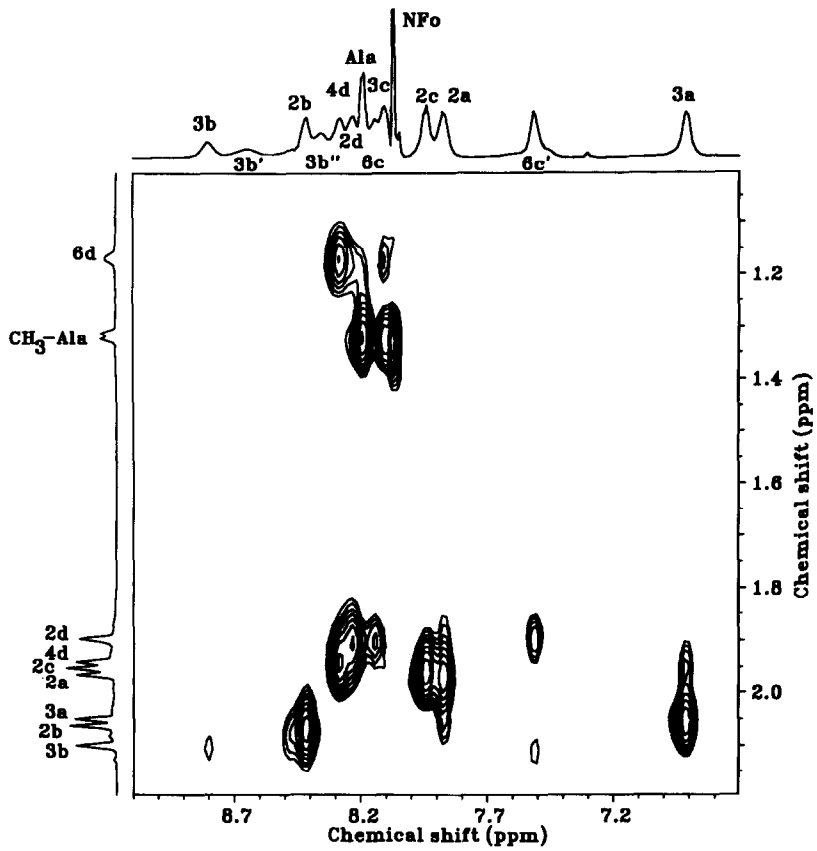

Fig. 6. 600 MHz NOESY spectrum, recorded at 27 °C in 90% H_2O–10% D_2O at pH 7.0, for the NH and CH_3 region of PS1 along with the corresponding one-dimensional spectra.

labelling of the glycose residues in OS2 was identical to the one for PS1 (Fig. 7). Since the ^1H resonances of OS2 due to its lower molecular weight were sharper than those for PS1 (Fig. 4), spin simulation of its ^1H spectrum was performed in order to refine coupling constants for the ring protons and confirm the configuration of the hexopyranoses (Table 3). Thus, the configuration for residue **a** was *galacto*; residue **b** *manno*; and residues **c** and **d** had the *gluco* configuration. For the NH resonances, coupling constants were measured directly from the spectra (Fig. 5c). The anomeric configuration for the *galacto*- and *gluco*-pyranosyl residues was determined from the magnitude of their vicinal coupling constants (Table 3). For the *manno*-pyranosyl residue the value of the $J_{1,2}$ coupling constant is close to 1 Hz for both α and β configurations. Occurrence of a single intraresidue NOE between H-1**a** and H-2**a** of PS1 established the α configuration for residue **a**. Presence of the intraresidue NOEs H-1/H-3 and H-1/H-5 for residues **b**, **c**, and **d** of PS1 confirmed their β configuration. NOEs were measured in the 2D mode, and the cross-sections through the NOESY spectrum of the PS1 are shown in Fig. 8.

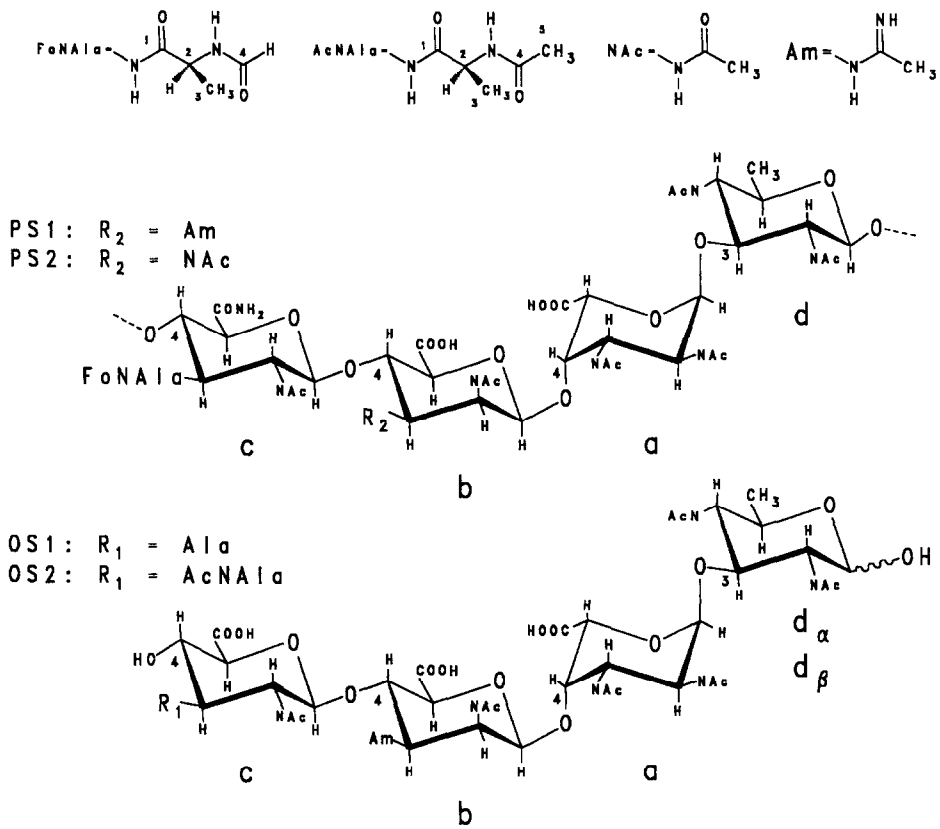

Fig. 7. Structures the PS1, PS2, OS1, and OS2 of *V. anguillarum* serotype O:2. (Abbreviations: FoNAla = *N*-formylated L-alanine; AcNAla = *N*-acetylated L-alanine.)

Table 3
$J_{H,H}$ coupling constants for OS2 of *V. anguillarum* serotype O:2 obtained from the spin simulated ^{1}H NMR spectrum [a,b]

H,H	Residue					
	a	**b**	**c**	**dβ**	**dα**	Ala
H-1,H-2	4.2	1.2	8.3	8.5	3.5	
H-2,H-3	8.3	3.1	11.2	10.0	10.0	7.3
H-3,H-4	3.9	9.8	9.8	10.0	10.0	
H-4,H-5	1.0	9.7	9.7	10.0	10.0	
H-5,H-6				6.2	6.3	
NH-2,H-2	9.8	9.5	9.8	9.9	9.8	6.2
NH-3,H-3	9.0	8.3	9.3			
NH-4,H-4				9.8	9.8	

[a] Recorded at 27 °C in D_2O at pH 7.0.
[b] NH protons spectrum was recorded at 27 °C in 90% H_2O–10% D_2O at pH 7.0.

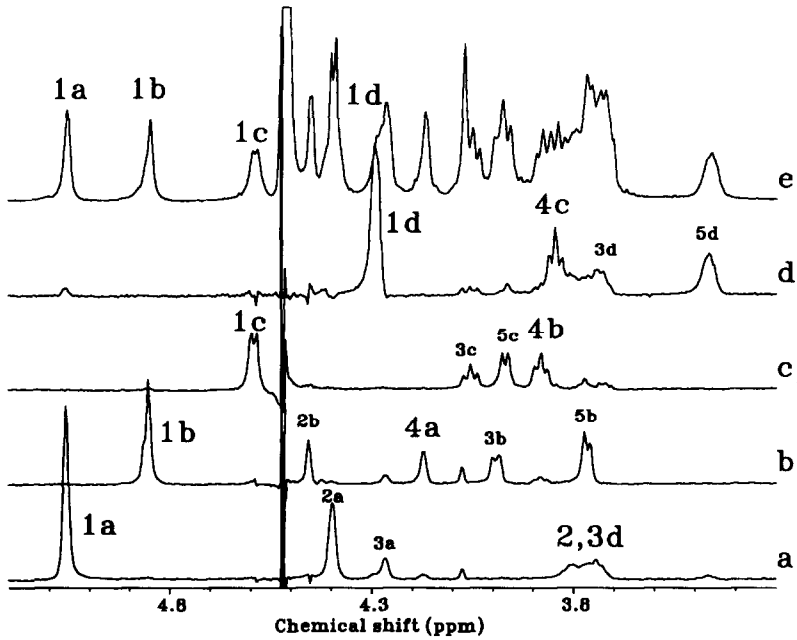

Fig. 8. Cross sections through 600 MHz NOESY spectrum of the PS1, recorded at 50 °C in D_2O at pH 7.0. Cross sections for: (a) H-1**a**; (b) H-1**b**; (c) H-1**c**; (d) H-1**d**. The observed ^1H NMR spectrum of PS1 is shown in (e).

Based on the NMR analysis and the chemical evidence, the following assignments of the monosaccharide residues were made: residue **a** was assigned to 2,3-diamino-2,3-dideoxy-α-galacturonic acid; residue **b** was assigned to 2,3-diamino-2,3-dideoxy-β-mannuronic acid; residue **c** was assigned to 2,3-diamino-2,3-dideoxy-β-glucuronic acid; residue **d** was assigned to 2,4-diamino-2,4,6-trideoxy-β-glucose.

Interresidue NOEs between H-1**a**/H-3**d**, H-1**b**/H-4**a**, H-1**c**/H-4**b**, and H-1**d**/H-4**c** established the sequence of the repeating unit of the PS1 as [-**c**-**b**-**a**-**d**]$_n$ (Fig. 8). Although other interresidue NOEs with the anomeric protons were observed, the linkage sites were clearly established as the only sites available for the formation of glycosidic linkages. In addition, a three-bond $^{13}C-^1H$ connectivity between C-1**c** and H-4**b**, and between C-4**a** and H-1**b** in the HMBC experiment confirmed the results of the NOE experiments.

Location of the N-*acetamidino group.*—The presence of an *N*-acetamidino group at C-3**b** was clearly confirmed by comparison of the NMR data from PS1 and PS2, obtained by treatment of PS1 with 5% triethylamine which resulted in conversion of the *N*-acetamidino group to an *N*-acetyl group [12,13]. Complete assignment the ^1H and ^{13}C spectrum of PS2 was also performed as outlined above for PS1. The observed loss of the characteristic ^{13}C resonances at 166.7 and 19.7 ppm and the absence of NH-3**b**″ and NH-3**b**″ resonances at 8.65 and 8.36 ppm in the ^1H NMR spectrum of PS2 (Fig. 5b) could be attributed to this conversion. In addition, a comparison of the ^1H and ^{13}C NMR

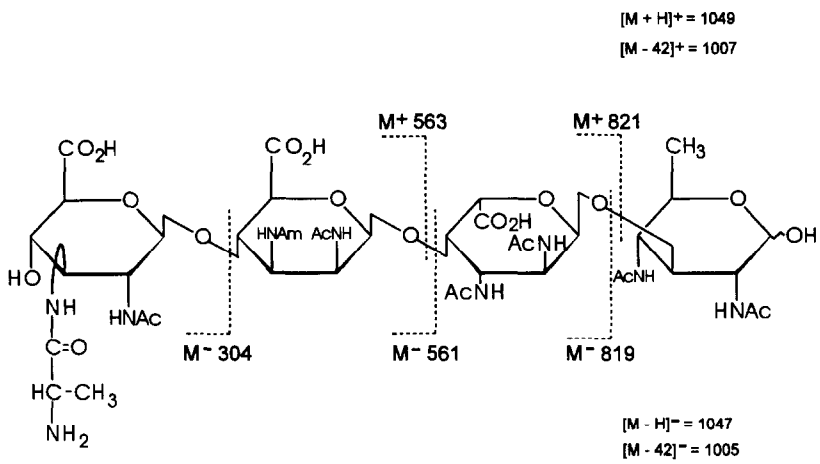

Fig. 9. Structure of the tetrasaccharide obtained during the partial hydrolysis of the PS1 from *V. anguillarum* serotype O:2 showing fragment ions obtained by FABMS in positive- and negative-ion mode.

data for PS1 and PS2 revealed differences in the chemical shifts of the NH-3**b**, NH-2**b**, H-3**b**, H-2**b**, C-3**b**, CH_3-3**b**, and CH_3-2**b** resonances (Tables 1 and 2).

Location of the alanine and N*-formyl groups.*—Presence of the intraresidue NOEs between the *N*-formyl proton and the C*H*, CH_3, and N*H* protons of alanine, as well as a long-range correlation with C-2 of alanine, indicated *N*-formylation of alanine in PS1.

N-Deformylation of PS2 resulted in the disappearance of the *N*-formyl proton at 8.08 ppm and caused shifts in the proton resonances of C*H* (−0.5 ppm) and CH_3 (+0.1 ppm) and ^{13}C resonances of *C*H (+0.9 ppm) and *C*H_3 (−1.4 ppm) of alanine from the corresponding resonances of alanine in PS2. A long-range correlation observed between the *C*H of alanine and H-3 of residue **c** in OS2 confirmed the *N*-formylation at position 3 of residue **c**. In addition, the NH-3**c**/C*H*-Ala and NH-3**c**/CH_3-Ala NOEs observed in PS1, PS2, and OS2 (Fig. 6) supported this conclusion.

Treatment of PS1 with 10 N HCl yielded a tetrasaccharide OS1 as a major oligosaccharide product. A ^{1}H NMR spectrum of OS1 indicated an absence of the *N*-formyl proton signal, confirming a complete *N*-deformylation. Consistent with the NMR evidence, the FABMS analysis of OS1 showed presence of molecular-ion species at *m*/*z* 1049 $[M + H]^+$ in the positive-ion mode and at *m*/*z* 1047 $[M - H]^-$ in the negative-ion mode (Fig. 9), further confirming these findings.

Location of the primary amide.—It was found that the carboxyl group of a residue **c** was in the form of a primary amide. The NH-6**c** and NH-6**c**′ resonances in PS1 and PS2 were assigned on the basis of their NOE to H-5**c** and NOE between NH-6**c** and NH-6**c**′. These signals disappeared after the mild acid treatment of PS2.

Absolute configuration of monosaccharides.—Only the absolute configuration of residue **d** (bacillosamine) could be determined by GLC–MS of the corresponding (*S*)-2-butyl glycoside derivative, and it was found to be D. The absolute configurations of the other monosaccharides were established by means of long-range NOEs involving the *N*-acetyl groups. NOEs have been previously used to establish the absolute

Table 4
Nuclear Overhauser enhancements used to determine the absolute configuration of monosaccharides in PS1 of *Vibrio anguillarum* serotype O:2. $R = (NOE_{ij}/NOE_{ix} * r_{ji}^6/r_{ix}^6)$, where r is the distance in Å obtained from the coordinates of the minimum-energy conformer of disaccharides with different absolute configurations

Linkage	H_i	-H_j	-H_x	NOE_{ij}	NOE_{ix}	r_{ij}	R(L–D)	R(D–D)
a–d	HN-2**d**	NAc-2**d**	H-1**a**	18	29	2.7	0.7	0.8
	HN-4**d**	NAc-4**d**	H-5**a**	11	23	2.7	0.9	0.1
	HN-4**d**	H-5**d**	H-3**a**	30	10	2.7	1.0	0.6
	NAc-4**d**	H-6**d**	H-5**a**	1	7	4.0	0.8	0.0
	HN-2**a**	NAc-2**a**	H-2**d**	17	20	2.6	0.5	0.2
							R(D–D)	R(D–L)
d–c	H-6**d**	H-5**d**	C*H*-Ala	6	3	2.5	1.6	0.1
	HN-3**c**	C*H*-Ala	H-6**d**	14	4	2.2	1.4	0.2
	NAc-2**d**	H-1**d**	H-5**c**	1	1	4.5	1.8	0.6
							R(D–L)	R(L–L)
b–a	H4**a**	H-5**a**	H-5**b**	43	12	2.5	1.1	1.1
	NAc-2**b**	H-2**b**	H-2**a**	1	2	4.6	1.4	0.4
	NAc-2**b**	H-2**b**	H-3**a**	1	1	4.6	0.8	0.3
	NAc-2**b**	H-2**b**	H-1**a**	1	0.5	4.6	1.1	1.2
							R(D–D)	R(D–L)
c–b	NAc-2**c**	CH_3-Ala	H-5**b**	4	1	2.9	1.6	0.7
	HN-2**b**	NAc-2**b**	H-1**c**	73	9	2.6	0.5	0.5

configurations of monosaccharides [14–16], and are a reliable method when more conventional methods are not amenable.

The absolute configuration of a monosaccharide is determined by performing the conformational analysis for each disaccharide linkage with two different absolute configurations for one of the component monosaccharides. The absolute configuration of the other monosaccharide must be known. Unique interglycosidic proton–proton constraints can thus be identified which are sometimes highly dependent on the relative absolute configuration of the monosaccharides. Conformational analysis showed that sugar residues could be quite constrained in their rotation about the glycosidic bond due to the presence of a large number of pendant groups around the pyranose ring. Thus, the minimum-energy conformer could be used to qualitatively analyse the NOEs.

NOE experiments were performed in 90% H_2O–10% D_2O solution in order to observe the NOE of the NH protons, which provided more constraints. The NOE, due to its sensitivity to interatomic proton distances (r^{-6}), was used to obtain constraints that are sensitive to the absolute configuration. Comparison of intraresidue NOEs, which are not affected by the absolute configuration of a sugar ring, to those of interresidue NOEs, permitted the identification of the absolute configuration (Table 4). Since, to a first approximation, $NOE_{ij} * r_{ij}^6 = NOE_{ix} * r_{ix}^6$, where NOE_{ij} and r_{ij} correspond to the NOE and distance for H_iH_j of the same residue, while NOE_{ix} and r_{ix} are those of the interresidue proton pair. For the correct absolute configuration, the ratio $(NOE_{ij}/NOE_{ix} * r_{ij}^6/r_{ix}^6)$ should be close to 1.

For the **a–d** linkage, the absolute configuration of residue **d** was known to be D from

chemical analysis. A number of NOEs were observed between the pendant *N*-acetyl groups, which were found to be highly sensitive to the absolute configuration of residue **a**. Hence, the significant NOEs for (HN-4**d**/H-5**a**), (HN-4**d**/H-3**a**), (NAc-4**d**/H-5**a**), and (HN-2**a**/H-2**d**) could only arise if residue **a** had the L configuration. For the D–D solution, the interproton distances were too big (> 4.5 Å) to satisfy these NOE constraints. Similarly, the absolute configuration of residue **c** could be determined from the observation of the (H-6**d**/C*H*-Ala), (HN-3**c**/H-6**d**), and (NAc-2**d**/H-1**d**) NOEs, which require residue **c** to have the D configuration, since only in the D–D configuration for linkage **d**–**c**, the interproton distances satisfied the NOE constraints. For the D–L configuration, these interproton distances are too large (> 5 Å), and none of the NOEs would have been observed. For linkage **b**–**a**, with the absolute configuration of residue **a** set as L, it was found that the D–L configuration for **b**–**a**, could satisfy the constraints imposed by the observed NOEs, since some distances where too large for the L–L configuration. The observed NOEs between **c**–**b** were found to be less sensitive to the relative configurations of their respective residues.

3. Discussion

In the present investigation, we established the structures of the O-chain and capsular polysaccharide from *Vibrio anguillarum* serotype O:2. Both capsular and O-chain polysaccharides have been shown by glycose analysis, partial hydrolysis, various specific modifications, one- and two-dimensional NMR spectroscopy and mass spectrometry methods to be high molecular weight polymers of a linear tetrasaccharide repeating unit (Fig. 7). In order to identify the nature and the position of the numerous nitrogen bearing groups present in the structure, the NMR experiments were also performed in H_2O. Potential-energy calculations in conjunction with conformational analysis were used to determine the absolute configurations of glycoses comprising the polysaccharide chains [14–16]. This method is useful when unusual monosaccharides are present and appropriate standards are not available to permit a more conventional analysis.

The repeating unit of these polysaccharides contains three different 2,3-diamino-2,3-dideoxy uronic acids and 2,4-diamino-2,4,6-trideoxy-D-glucose, bacillosamine, previously found in several bacterial polysaccharides. 2,3-Diacetamido-2,3-diamino-2,3-dideoxy-L-galacturonic acid was previously found in the LPS from *Bordetella parapertussis* and *B. bronchiseptica* [17]. 3-Acetamidino-2-acetamido-2,3-dideoxy-D-mannuronic acid was identified in several O-polysaccharides from *Pseudomonas aeruginosa* [12]. 2,3-Diacetamido-2,3-dideoxy-D-glucuronic acid was reported in the O-polysaccharide from *P. aeruginosa* serotype O:6 [18,19] and is a component of *Thiobacillus* sp. IFO 14570 O-antigen [20]. However, this is the first time the *N*-formyl-L-alanyl group has been identified in bacterial polysaccharides.

So far, very limited structural data has been available on the lipopolysaccharides from *V. anguillarum* [21–24]. Although preliminary investigations by Tajima et al. have demonstrated presence of a capsule in many strains of *V. anguillarum* [7], this is the

first definitive report on the composition and structure of the capsular polysaccharide from a *Vibrio* species.

4. Experimental

Bacterial culture.—*Vibrio anguillarum* serotype O:2 strain ATCC 19264 [25] was grown in brain heart infusion (BHI) broth (Difco) containing 1.5% NaCl in a 75L IF-75 fermenter (New Brunswick Scientific) at 19 ± 1 °C overnight (~ 18 h) and harvested in 1% phenol solution.

Extraction and purification of capsular polysaccharide (PS1) [8].—Bacterial cells (660 g, wet weight) were washed with 2.5% saline and resuspended in 1.8 L of phosphate buffer (0.1 M, pH 7.0) containing 5 mM EDTA, 0.02 M sodium azide and egg-white lysozyme (400 mg, Sigma). The suspension was continuously stirred at 4 °C overnight. The cells were removed by low-speed centrifugation and used for the isolation of lipopolysaccharide. The clear supernatant was dialysed against distilled water and concentrated. Nucleic acids were removed by precipitation with ethanol (25%, v/v) and $CaCl_2$ (0.1 M). The capsular polysaccharide was precipitated from the solution by increasing the ethanol concentration to 80% (v/v). The precipitate was dissolved in water, dialysed, and lyophilized to give a crude PS1 (yield, 890 mg). It was applied to a Sephadex G-100 column in three portions, and void-volume fractions were collected (270 mg). Further purification was achieved by gel-filtration chromatograpy on a Sepharose 6B column. The main fraction was collected, dialysed and lyophilized to afford purified PS1 (yield, 220 mg).

Isolation of LPS and preparation of O-chain polysaccharide.—Washed cells of *V. anguillarum* strain ATCC 19264 were extracted by the method of Westphal et al. [9], and an aqueous-phase LPS was purified by repeated ultracentrifugation (yield 5.1 g). The water-phase LPS was heated with 3% aq acetic acid (3 h, 100 °C) and, following the removal of the insoluble lipid A by low-speed centrifugation (5000 *g*, 10 min, 4 °C), the clear supernatant lyophilized and applied to a Sephadex G-100 column. Fractions containing glucan, O-chain polysaccharide, and core oligosaccharide were collected and lyophilized.

SDS–PAGE.—LPS preparations were subjected to SDS–PAGE with the Laemmli buffer system [26]. The 4% stacking gel and the 12.5% separating gel did not contain SDS [27].

Treatment of PS1 with triethylamine [12,13].—PS1 (15 mg) was treated with 5% triethylamine (3.5 h, 70 °C). The solution was coevaporated four times with water and lyophilized. Further purification on a Sephadex G-100 column afforded a modified polysaccharide PS2 in which the *N*-acetamidino group had been converted to an *N*-acetyl group (yield, 6 mg).

N-*Deformylation of PS2 [28].*—PS1 (20 mg) was treated with 5% triethylamine as described above, and the residue was heated with 0.05 M HCl (4 mL, 4.5 h, 105 °C). The product was purified by gel filtration on a Sephadex G-50 column to give a *N*-deformylated PS2 (yield, 10 mg).

Carbodiimide reduction of PS1 [29].—PS1 (30 mg) was dissolved in distilled water (10 mL), and the pH was adjusted to 4.7 with 0.05 N NaOH. After addition of 1-cyclohexyl-3-(2-morpholinoethyl)carbodiimide metho-*p*-toluenesulfonate (130 mg), the stirred mixture was maintained at pH 4.7 with 0.05 N HCl. When the consumption of hydrochloric acid ceased, sodium borohydride (10% w/v, 600 mg) was added, the pH of the solution was maintained at 7.0 for 2 h, and then the reaction was allowed to proceed for 17 h at room temperature. The mixture was neutralized with dilute acetic acid, dialysed extensively against distilled water, and lyophilized. The residue was subjected to a repeated carbodiimide reduction following the procedure described above. The product was first subjected to ion-exchange chromatography on a DEAE-Sephacel column, and the neutral fraction was further purified by gel filtration on a Sephadex G-100 column. The void volume peak was collected to afford a carbodiimide-reduced PS1 (yield, 7 mg).

Partial hydrolysis of PS1: preparation of OS1 and OS2.—PS1 (12 mg) was dissolved in 10 N HCl (4 mL) and heated for 15 min at 90 °C. The reaction mixture was cooled, and hydrochloric acid was removed by a co-evaporation with distilled water (five times). The residue was neutralized with dilute ammonium hydroxide and purified on a column of Bio-Gel P-2 to afford oligosaccharide OS1 as a major product (yield, 3 mg).

To prepare OS2, PS1 (22 mg) was hydrolysed with 10 N HCl as described above, and the residue was dried in vacuo over P_2O_5. It was dissolved in dry methanol (3 mL), and acetic anhydride (300 μL) and pyridine (60 μL) were added. The reaction was carried out for 1 h at room temperature, and after the evaporation, the residue was fractionated on a Bio-Gel P-2 column to give oligosaccharide OS2 (yield, 6 mg).

Analytical methods.—Glycoses were determined by GLC as their alditol acetates. A sample of a carbodiimide-reduced PS1 was treated with 10 N HCl at 95 °C for 15 min, and the hydrolysate was subjected to *N*-acetylation [30], followed by reduction ($NaBD_4$) and acetylation. The absolute configuration of 2,4-diamino-2,4,6-trideoxy-glucose was determined by GLC of its acetylated (*S*)-2-butylglycoside derivative and confirmed by comparison of its GLC retention time and MS with that of the authentic sample [31]. The absolute configuration of alanine was confirmed by comparison of the GLC retention time and MS of the *N*-acetyl-(*R*)-2-octyl ester with those of an authentic standard. The absolute stereochemistry of the remaining glycoses was determined by means of long-range NOEs involving the *N*-acetyl groups (see below). GLC analysis was performed with a Hewlett–Packard Model 5710 A gas chromatograph fitted with a hydrogen flame ionizer using a fused-silica capillary column (0.3 mm × 25 m) containing 3% OV 17; an initial column temperature of 180 °C was held for 2 min, followed by an increase to 240 °C at 4 °C/min. Fast-atom bombardment mass spectra (FABMS) were acquired on a JEOL AX5O5H double-focusing mass spectrometer operating at an accelerating voltage of 3 kV and analysed as previously described [32].

Samples were methylated according to the method of Ciucanu and Kerek [33], and, following hydrolysis with 4 M trifluoroacetic acid (120 °C, 1 h), the reduced ($NaBD_4$) and acetylated products were analysed by GLC–MS.

Gel-filtration chromatography of polysaccharides was carried out on columns of Sephadex G-50 (1.0 × 70 cm) and Sephadex G-100 (2.6 × 90 cm) (Pharmacia Fine Chemicals, Uppsala, Sweden) irrigated with 0.02 M pyridinium acetate (pH 5.6) or

Sepharose 6B (2.6 × 90 cm) column (Pharmacia Fine Chemicals, Uppsala, Sweden) irrigated with 1/30 M phosphate butter (pH 8.0). Separations of oligosaccharides were made on a column of Bio-Gel P-2 (2.6 × 90 cm) (Bio-Rad, USA) irrigated with 0.02 M pyridinium acetate butter (pH 5.6). Column eluates were continuously monitored using a Waters R403 differential refractometer, and samples (100 μL) were analysed colorimetrically for aldose [34] and aminoglycose [35].

The gel-filtration properties of the eluted materials are expressed in terms of their distribution coefficient K_{av}. $K_{av} = (V_e - V_0)/(V_t - V_0)$, where V_e is the elution volume of the specific material, V_0 is the void volume of the system and V_t is the total volume of the system.

Ion-exchange chromatography of the carbodiimide-reduced O-polysaccharide was performed on a column (1.2 × 22 cm) of DEAE-Sephacel (Pharmacia Fine Chemicals, Uppsala, Sweden) equilibrated with 0.01 M NaCl in distilled water. Optical rotations were determined at 20 °C in 10-cm tubes using a Perkin–Elmer Model 243 polarimeter.

NMR spectroscopy.—^{1}H and ^{13}C NMR spectra were recorded with a Bruker AMX 500 or AMX 600 spectrometer using standard Bruker software. Spectra of D_2O solutions were recorded at 50 °C for the polysaccharides PS1 and PS2 and at 27 °C for the oligosaccharide OS2 at concentrations of 5 mg in 0.5 mL of D_2O. For the detection of NH protons, spectra were recorded at 27 °C in 90% H_2O–10% D_2O. Samples of PS1 and PS2 were dissolved in 10 mM phosphate buffer pH 7.0, followed by two lyophilizations with D_2O. Oligosaccharide OS2 was dissolved in distilled water, and the pH was adjusted to 7.0 with 10 mM NaOH, followed by two lyophilizations with D_2O.

All NMR experiments were performed using a 5 mm broadband probe with ^{1}H coil nearest to the sample. Acquisition and processing of respective 2D NMR experiments, and spin simulations were done as described previously [13]. The observed ^{1}H chemical shifts are reported relative to internal acetone (2.225 ppm), and the ^{13}C chemical shifts are quoted relative to the methyl group of internal acetone (31.07 ppm).

Potential energy calculations.—The coordinates of the glycosides were generated from the coordinates of mannose, galactose, and glucose, and modified with Alchemy II (Tripos Associates, Inc.). The coordinates of the methyl glycosides were then refined by molecular mechanics calculations using MM3(92) [36]. Conformational analysis was done using PFOS potential [37] as described before [15].

Acknowledgements

We thank Mr. Fred Cooper for the expert GLC–MS and FABMS analyses and Mr. D.W. Griffith for the production of bacterial cells.

References

[1] P.D. Smith, in A.E. Ellis (Ed.), *Fish Vaccination*, Academic Press, London, 1988, pp 67–84.
[2] R.E. Pacha and E.D. Kiehn, *J. Bacteriol.*, 100 (1969) 1242–1247.
[3] U.B.S. Sørensen and J.L. Larsen, *Appl. Environ. Microbiol.*, 51 (1986) 593–597.

[4] H.B. Rasmussen, *Curr. Microbiol.*, 16 (1987) 39–42.
[5] H. Chart and T.J. Trust, *Can. J. Microbiol.*, 30 (1984) 703–710.
[6] L.M. Mutharia and P.A. Amor, *FEMS Microbiol. Lett.*, 123 (1994) 289–298.
[7] K. Tajima, Y. Ezura, and T. Kimura, *Fish Pathol.*, 22 (1987) 221–226.
[8] S.D. Elliott and J.Y. Tai, *J. Exp. Med.*, 148 (1978) 1699–1704.
[9] O. Westphal and K. Jann, *Methods Carbohydr. Chem.*, 5 (1965) 83–91.
[10] L. Kenne, B. Lindberg, E. Schweda, B. Gustafsson, and T. Holme, *Carbohydr. Res.*, 180 (1988) 285–294.
[11] Y.A. Knirel, A.S. Vinogradov, A.S. Shashkov, B.A. Dmitriev, N.K. Kochetkov, E.S. Stanislavsky, and G.E. Mashilova, *Eur. J. Biochem.*, 163 (1987) 627–637.
[12] Y.A. Knirel, N.A. Paramonov, E.V. Vinogradov, A.S. Shashkov, B.A. Dmitriev, N.K. Kochetkov, E.V. Kholodkova, and E.S. Stanislavsky, *Eur. J. Biochem.*, 167 (1987) 549–561.
[13] K. Hermansson, M.B. Perry, E. Altman, J.R. Brisson, and M.M. Garcia, *Eur. J. Biochem.*, 212 (1993) 801–809.
[14] H. Baumann, A.O. Tzianabos, J.R. Brisson, D.L. Kasper, and H.J. Jennings, *Biochemistry*, 31 (1992) 4081–4089.
[15] M. Kulakowska, J.R. Brisson, D.W. Griffith, M. Young, and H.J. Jennings, *Can. J. Chem.*, 71 (1993) 644–648.
[16] V. Pavliak, D. Uhrin, J.R. Brisson, A.O. Tzianabos, D.L. Kasper, and H.J. Jennings, *Carbohydr. Res.*, 275 (1995) 333–341.
[17] J.L. Di Fabio, M. Caroff, D. Karibian, J.C. Richards, and M.B. Perry, *FEMS Lett.*, 97 (1992) 275–282.
[18] Y.A. Knirel, N.A. Kocharova, A.S. Shashkov, B.A. Dmitriev, and N.K. Kochetkov, *Carbohydr. Res.*, 93 (1981) C12–C13.
[19] B.A. Dmitriev, N.A. Kocharova, Y.A. Knirel, A.S. Shashkov, N.K. Kochetkov, E.S. Stanislavsky, and G.M. Machilova, *Eur. J. Biochem.*, 125 (1982) 229–237.
[20] A.S. Shashkov, S. Campos-Portuguez, H. Kochanowski, A. Yokota, and H. Mayer, *Carbohydr. Res.*, 269 (1995) 157–166.
[21] J.H. Banoub, F. Michon, and F. Cooper, *Can. J. Biochem. Cell. Biol.*, 63 (1985) 1265-1267.
[22] J.H. Banoub, F. Michon, and H.J. Hodder, *Biochem. Cell. Biol.*, 65 (1987) 19–26.
[23] H. Eguchi, S. Kaya, and Y. Araki, *Carbohydr. Res.*, 231 (1992) 147–158.
[24] H. Eguchi, S. Kaya, and Y. Araki, *Carbohydr. Res.*, 231 (1992) 159–169.
[25] J. Bagge and O. Bagge, *Nord. Veterinaemed. Bb.*, 8 (1956) 481–492.
[26] U.K. Laemmli and M. Favre, *J. Mol. Biol.*, 80 (1973) 575–599.
[27] P.J. Hitchcock and T.M. Brown, *J. Bacteriol.*, 154 (1983) 269–277.
[28] Y.A. Knirel, E.V. Vinogradov, A.S. Shashkov, N.K. Kochetkov, B.A. Dimitriev, E.S. Stanislavsky, and G.M. Mashilova, *Eur. J. Biochem.*, 150 (1985) 541–550.
[29] R.L. Taylor and H.E. Conrad, *Biochemistry*, 11 (1972) 1383–1388.
[30] B. Kozulic, B. Ries, and P. Midner, *Anal. Biochem.*, 94 (1979) 36–39.
[31] G.J. Gerwig, J.P. Kamerling, and J.F.G. Vliegenthart, *Carbohydr. Res.*, 77 (1979) 1–7.
[32] H. Masoud, E. Altman, J.C. Richards, and J.S. Lam, *Biochemistry*, 33 (1994) 10568–10578.
[33] I. Ciucanu and F. Kerek, *Carbohydr. Res.*, 131 (1984) 209–217.
[34] M. Dubois, K.A. Gilles, J.K. Hamilton, P.A. Rebers, and F. Smith, *Anal. Chem.*, 28 (1956) 350–356.
[35] A. Tsuji, T. Kinoshita, and M. Hoshino, *Chem. Pharm. Bull.*, 17 (1968) 217–219.
[36] U. Burket and N.L. Allinger, *Molecular Mechanics*, ACS monograph 177, American Chemical Society, Washington, DC, 1982.
[37] I. Tvaroska and S. Pérez, *Carbohydr. Res.*, 149 (1986) 389–410.